



Oil Palm Fronds Activated Carbon via Microwave-assisted H₃PO₄ Activation: Box-Behnken Optimization for Crystal Violet Dye Removal

Nur Atirah Shamsudin

Soil Assessment and Remediation Research Group, Faculty of Applied Sciences, Universiti Teknologi MARA, Selangor, Malaysia

Qistina Omar

Soil Assessment and Remediation Research Group, Faculty of Applied Sciences, Universiti Teknologi MARA, Selangor, Malaysia; AND Centre of Foundation Studies, Universiti Teknologi MARA, Cawangan Selangor, Kampus Dengkil, Dengkil 43800, Selangor, Malaysia

Ismaniza Ismail

Soil Assessment and Remediation Research Group, Faculty of Applied Sciences, Universiti Teknologi MARA, Selangor, Malaysia

Noor Artika Hassan

Department of Community Medicine, Kulliyah of Medicine, International Islamic University Malaysia, Kuantan, Pahang, Malaysia

Syarifah Abd Rahim

Faculty of Chemical & Process Engineering Technology, College of Engineering Technology, Universiti Malaysia Pahang, 26300 Gambang, Pahang, Malaysia

Nur Fazreen Dzulkafli

Department of Science and Biotechnology, Faculty of Engineering and Life Sciences, Universiti Selangor, Jalan Timur Tambahan, 45600, Selangor, Malaysia

Ruihong Wu

Soil Assessment and Remediation Research Group, Faculty of Applied Sciences, Universiti Teknologi MARA, Selangor, Malaysia

Soon Kong Yong

Soil Assessment and Remediation Research Group, Faculty of Applied Sciences, Universiti Teknologi MARA, Selangor, Malaysia

Follow this and additional works at: <https://acbs.alayen.edu.iq/journal>



Part of the [Biology Commons](#), [Biotechnology Commons](#), and the [Medicine and Health Sciences Commons](#)

Recommended Citation

Shamsudin, Nur Atirah; Omar, Qistina; Ismail, Ismaniza; Hassan, Noor Artika; Rahim, Syarifah Abd; Dzulkafli, Nur Fazreen; Wu, Ruihong; and Yong, Soon Kong (2024), Oil Palm Fronds Activated Carbon via Microwave-assisted H₃PO₄ Activation: Box-Behnken Optimization for Crystal Violet Dye Removal, *AUIQ Complementary Biological System*: Vol. 1: Iss. 1, 77-88.

DOI: <https://doi.org/10.70176/3007-973X.1008>

Available at: <https://acbs.alayen.edu.iq/journal/vol1/iss1/9>



ORIGINAL STUDY

Oil Palm Fronds Activated Carbon via Microwave-assisted H_3PO_4 Activation: Box-Behnken Optimization for Crystal Violet Dye Removal

Nur Atirah Shamsudin ^a, Qistina Omar ^{a,b}, Ismaniza Ismail ^a, Noor Artika Hassan ^c,
Syarifah Abd Rahim ^d, Noor Fazreen Dzulkafli ^e, Ruihong Wu ^f, Soon Kong Yong ^{d, a,*}

^a Soil Assessment and Remediation Research Group, Faculty of Applied Sciences, Universiti Teknologi MARA, Selangor, Malaysia

^b Centre of Foundation Studies, Universiti Teknologi MARA, Cawangan Selangor, Kampus Dengkil, Dengkil 43800, Selangor, Malaysia

^c Department of Community Medicine, Kulliyyah of Medicine, International Islamic University Malaysia, Kuantan, Pahang, Malaysia

^d Faculty of Chemical & Process Engineering Technology, College of Engineering Technology, Universiti Malaysia Pahang Al-Sultan Abdullah, Gambang, 26300, Pahang, Malaysia

^e Department of Science and Biotechnology, Faculty of Engineering and Life Sciences, Universiti Selangor, Jalan Timur Tambahan, 45600, Selangor, Malaysia

^f Department of Chemistry, Hengshui University, 053500, Hengshui, Hebei Province, China

ABSTRACT

The extensive use of crystal violet (CV) dyes may cause water pollution. A highly porous and functionalized activated carbon can be used for adsorption of CV dyes. Activated carbon was prepared from oil palm fronds through microwave-assisted pyrolysis and activation with phosphoric acid (H_3PO_4) for removal of CV dye from wastewater. The physico-chemical characteristics of oil palm fronds activated carbon (OPFAC) was employed by Brunauer-Emmett-Teller (BET) surface area analysis, Fourier transform infrared (FT-IR) analysis, Scanning Electron Methodology-Energy Dispersive X-Ray (SEM-EDX) analysis, thermogravimetric analysis (TGA), and point of zero charges (pH_{pzc}). The adsorption parameters such as pH (4, 7, and 10), dosage (0.02, 0.06, and 0.1 g), and contact time between adsorbent and adsorbate (2, 5, and 8 mins) were optimized using the response surface methodology-Box-Behnken design (RSM-BBD). The experimental results showed that the optimum conditions for the removal of CV dye by OPFAC were 0.1 g dosage, pH 9, contact time of 5 min with the percentage removal of CV dye is 91.4%. The adsorption capacity of OPFAC for CV dye was well fitted by the pseudo-second-order (PSO) kinetic model. The maximum adsorption capacity (q_{max}) from Langmuir isotherm was 188.4 mg/g. The isotherm study is well described by Freundlich model with coefficient of correlation ($R^2 = 0.9488$) describe that the CV dye adsorption occurred multilayer adsorption onto heterogenous adsorption site. The thermodynamics study indicated that the adsorption process of OPFAC is through spontaneous and endothermic condition as the values of ΔH° (21.86 KJ/mol) and ΔS° value (87.90 J/mol K) is positive.

Keywords: Oil palm frond, Activated biochar, Microwave pyrolysis, Activated carbon

1. Introduction

Palm oil is considered one of the largest crops in Malaysia, with an area of around 5.65 million hectares in Malaysia in 2023 [1, 2]. The rapid growth

of oil palm plantations produces a large amount of biomass from oil palm trees. The biomass comes from oil palm shells (OPS), empty fruit bunches (EFB), palm oil mill effluent (POME), oil palm trunk (OPT), and oil palm fronds (OPF). Unlike OPT, EFB, OPS, and

Received 24 April 2024; accepted 10 July 2024.
Available online 2 August 2024

* Corresponding author.
E-mail address: yongsk@uitm.edu.my (S. K. Yong).

<https://doi.org/10.70176/3007-973X.1008>

3007-973X/© 2024 Al-Ayen Iraqi University. This is an open access article under the CC BY-NC-ND license (<http://creativecommons.org/licenses/by-nc-nd/4.0/>).

POME, there are no significant commercial applications for the OPF. In general, 24% of OPF is harvested from each oil palm tree in a year. In 2022, 59.593 million tons of dry OPF were produced in Malaysia. About 15 tons of dry OPF per hectare are usually trimmed off and left to degrade naturally in the field during the replanting seasons. Oil palm fronds can be a ruminant feed. However, OPF contains high levels of neutral detergent fibre (NDF) and lignin that can lead to a low level of ruminant digestibility [3, 4]. The chemical compositions of OPF are 36% hemicellulose, 35% cellulose, and 29% lignin. The OPF is a potential raw material for producing biochar or activated carbon through pyrolysis and impregnation processes for wastewater treatment. In the simplest word, it can be converted into a valuable product. Palm kernel shells (PKS) are usually used in many studies. However, the high demand from Japan, Korea, China, and Thailand for PKS as fuel has increased its price. The cheaper OPF can be a good substitute for PKS as feedstock for producing sorbent.

The presence of dye from the textile, paper, leather, pharmaceutical, and food industries can lead to water pollution. The discharge of dyes to water bodies may cause health problems to the human and aquatic ecosystem. Crystal violet (CV) is the common dye used in the textile and paper industries. Despite of widely used, CV has been identified as a carcinogenic compound. Exposure to the <1 ppm of CV dyes can cause respiratory problem, kidney damage, and blandness. If exposure is increased to more than that, irritation to the skin and the digestive system may occur [5]. Nonetheless, CV has a complex chemical structure and is persistent in the environment, having a low degradability and high solubility in water. Therefore, there is a need for removing CV dyes from the water bodies.

There are several methods for removing CV dyes from the environment, such as membrane filtration, advanced oxidation, biological degradation, photocatalysis, and absorption. Biological treatment is considered an environmentally friendly and cost-effective approach, but it is very time-consuming and ineffective. Therefore, adsorption is one of the prevalent methods for eliminating pollutants from wastewater. The common adsorbents for adsorption are activated carbon and biochar. Activated carbon is a cost-effective, environmentally friendly, effective, and fast-acting sorbent. However, commercial activated carbon is costly. Agricultural waste has been used in the production of activated carbon because of its abundance, low environmental impact, low cost, and renewability [3].

The extensive use of dyes may cause water pollution when their residue may lead to groundwater-

surface. Contaminating groundwater with dyes makes it unsuitable for use and harms the non-target organism. The OPF is a cost-free solid waste from the oil palm trees. OPF is converted to activated carbon using a pyrolysis process which requires higher temperature, higher energy, and long processing time. Therefore, this study aims to solve the problem by converting OPF into activated carbon using the microwave method. Microwaves can provide uniform heating, shorter processing times, and higher energy saving [6].

Phosphoric acid may convert OPF into porous activated carbon. The phosphoric acid first reacts with cellulose and lignin in lignocellulose as cellulose is resistant to hydrolysis of acid. The evaporation of phosphoric acid during the carbonization process creates more pores and increases the number of pores on the surface of activated carbon [7]. The mechanism of phosphoric acid in converting OPF into porous activated carbon are depolymerisation, dehydration, and redistribution of biopolymers in biomass materials. Therefore, porous activated carbon with high porosity and good functionality can act as an effective adsorbent for the adsorption of CV dyes. The porosity and functionality of OPF activated carbon are dependent on the surface characteristic of activated carbon. The adsorption of CV dye onto the adsorbent is influenced by van der Waals forces, hydrogen bonding, cation- π interaction, and electrostatic interaction [8].

In this study, OPF activated carbon was produced using phosphoric acid as activating agent and then physically activated by microwave pyrolysis. Optimum adsorption condition of CV dye on OPF activated carbon was first studied using the response surface methodology-Box-Behnken design (RSM-BBD). The adsorption data was analysed using various kinetic, isotherm, and thermodynamic models for elucidating the sorption performance and mechanisms of CV dye on OPF activated carbon.

2. Methodology

This study only used optimum parameters for preparation of activated carbon such as radiation time (15 min), microwave power (800 W), mixing ratio (1g OPF: 2 mL H₃PO₄), and particle size of OPFAC (250 μ m). The characteristic of OPFAC then has been identified in terms of FT-IR analysis, SEM-EDX analysis, thermogravimetric analysis (TGA), and point of zero charges (pH_{pzc}). The optimization adsorption study parameter such as pH (4, 7, and 10), dosage (0.02, 0.06, and 0.1), and contact time between absorbance and adsorbate (2, 5, and 8 mins) were conducted using response surface

methodology-Box-Behnken design (RSM-BBD) based on a preliminary test. To investigate the effectiveness of OPFAC in terms of percentage removal of CV dye. The adsorption studies were conducted using kinetic, isotherm, and thermodynamic models.

All the chemicals and materials used in this experiment from the laboratory of preparation chemical lab (A105) except oil palm fronds. Oil palm frond (OPF) was collected from a local oil palm field in Gua Musang, Kelantan. The concentrated of phosphoric acid was used during activation time by impregnated OPF for 30 min with a constant ratio of 1g OPF: 2 mL H₃PO₄. The 1M sodium hydroxide and 1M hydrochloric acid were used in the pH adsorption study.

All the instruments used for this experiment were from the laboratory of Faculty of Applied Sciences. The crusher was used for crushed oil palm fronds. The oven (TR 240) was used for the drying process of OPF, microwave (SAMSUNG Solo 20 L Microwave oven ME711K) was used for the preparation of activated carbon. Brunauer-Emmett-Teller (BET) surface area of the OPFAC was examined using the surface area analyzer (ASAP 2060, Micromeritics). The Fourier-transform infrared spectroscopy (Perkin-Elmer RX I) was used to identify the functional group in OPFAC. Then, a scanning electron microscope (SEM, Zeiss Supra 40 VP) was used to investigate the morphology structure of OPFAC. The UV-VIS spectrometer (PG Instrument, Model 70+) was used for the adsorption study of crystal violet on OPFAC.

2.1. Preparation of activated carbon

Oil Palm Fronds (OPF) were collected from a local oil palm field in Gua Musang, Kelantan. Firstly, OPF was crushed into small sizes using a crusher. Next, OPF was washed with boiling water several times to remove impurities and then was placed into a drying oven at 100°C for 24 h to remove the moisture. The dried OPF was carbonized using a microwave oven for 15 min at 800 W under 2 L/min N₂ gas flow. After that, OPF was impregnated with phosphoric acid with a constant ratio of 1 g OPF: 2 mL H₃PO₄ and dried in the oven for 24 h at 100°C. After oven drying, OPF was placed into the microwave oven with radiation power of 800 W for 15 min under 2 L/min N₂ gas flow. Then, OPFAC was rapidly rinsed with boiling distilled water until the solution became neutral. The OPFAC was then placed in the oven at 100°C for 24 h to remove the moisture. Lastly, the OPFAC was sieved to a consistent particle size of 250 μm. The OPFAC was placed in a sealed container to avoid contamination and moisture content. The percentage

yield of the OPFAC was calculated with Eq. (1):

$$\text{Yield (\%)} = \frac{\text{Wt. of OPAC}}{\text{Wt. of dried OPF}} \times 100 \quad (1)$$

2.2. Characterization of OPFAC

Four experiments were conducted in the characterization of OPFAC, which are SEM-EDX analysis, FT-IR analysis, TGA analysis, and point of zero charges. The functional group of OPFAC was identified using FT-IR spectrometer (Perkin Elmer Spectrum One FTIR). The transparent cell was prepared by mixing 0.09g of KBr with 0.01g of OPFA in a mortar. The mixture was pressed with the hydraulic pump to get a transparent and thin solid plate and was then transferred to the FTIR analyser. The FTIR study on OPFAC was carried out in the range of 4000 to 500 cm⁻¹ with 4 cm⁻¹ resolution and 4 scans. The bands were labelled according to the functional groups in OPFAC. The procedure was repeated for the OPFAC after adsorption of CV dye to analyse the changes of functional group after adsorption. The high spectral resolution data of OPFAC was compared and analysed for their relation with the adsorption of CV dye.

The scanning electron microscope-energy dispersive X-ray (SEM-EDX, Zeiss Supra 40 VP, Germany) was used to investigate the morphology structure of OPFAC. The sample was sputtered on carbon tape and placed in the chamber, where the image of the morphology sample was taken using the SEM method. Thus, the sample was magnified to 1000x, 2500x, and 7000x using ZEISS SmartSEM software. This step was repeated after the adsorption of CV dye. After the SEM analysis were conducted, EDX analysis were also evaluated using the same method.

The purposed of this study to identified the degree of thermal degradation and stability of OPFAC. The analysis was conducted using thermogravimetric analyser. The experiment was carried out with about 0.100 mg of OPF and increased temperature from room temperature to 600°C at heating rate 10°C.min⁻¹.

The point of zero charge (pH_{pzc}) was determined according to method described by Mahdi, Hanandeh [9]. Exactly 0.1 g of OPFAC was mixed with 100 mL of 0.1 M NaCl solution with the range pH between 3 to 11 adjusted by 0.1 M of HCl and NaOH solution. The solution was shaken in a rotary shaker for 24 h at room temperature. After that, the final pH of the solution was measured. The ΔpH was than calculated with Eq. (2):

$$\Delta\text{pH} = \text{Final pH} - \text{Initial pH} \quad (2)$$

Table 1. Codes and range of independent variable with their codes.

Codes	Variables	Level 1 (−1)	Level 2 (0)	Level 3 (+1)
A	Dose (g)	0.02	0.06	0.1
B	pH	4	7	10
C	Time (min)	2	5	8

2.3. Optimization condition study

Three independent variables which are dosage, pH, and contact time were optimized using Box-Behnken design (BBD) in response surface methodology (RSM) for the crystal violet (CV) dye adsorption onto OPFAC. The experiments were designed with Design-Expert software using preliminary test results. A total of 17 experiments are designed by BBD to optimize and evaluate the three variable which is adsorbent dosage (0.02, 0.06, and 0.1 g), pH (4, 7, and 10), and contact time (2, 5, and 8 min) on the CV dye removal. The level and range of independent variables are shown in Table 1 with their codes. The actual experiment design and value of CV dye removal are given in Table 2. A certain amount of OPFAC was added into a 125 mL Erlenmeyer flask containing 100 mL CV dye solution. These flasks were agitated at a fixed shaking speed (150 strokes/min) using a rotary shaker. After that, the solution was filtered by a syringe filter (0.22 μm). Finally, the concentration of CV dye was measured by UV-Vis spectroscopy at λ_{max} 590 nm. The percentage of CV dye removal was calculated using Eq. (3):

$$\text{CV}\% = \frac{C_o - C_e}{C_o} \times 100 \quad (3)$$

where C_o (mg/L) is the CV dye initial concentration and C_e (mg/L) is the concentration of final reading of CV dye at equilibrium.

2.4. Batch sorption experiments

The CV dye adsorption onto OPFAC was conducted in batch mode study. The optimum condition of adsorption study key parameter was kept constant in the concentration study experiment, which is the adsorbent dose 0.1 g and pH 9. The adsorption experiment of CV dye was conducted using the same procedures as above [3.6] at different concentrations of CV dye (50, 100, 150, 200, 250, and 300 ppm) and contact time (1–240 min). The adsorption capacity of OPFAC for CV dye at equilibrium, q_e (mg/g) was identified using Eq. (4):

$$q_w = \frac{(C_o - C_e)V}{W} \quad (4)$$

Table 2. The 3-variables BBD matrix and experimental data for CV removal efficiency.

Std	Run	A: Dose (g)	B: pH	C: Time (min)	CV removal (%)
1	5	0.02	4	5	27.8
2	17	0.1	4	5	87.4
3	13	0.02	10	5	51.9
4	9	0.1	10	5	91.4
5	7	0.02	7	2	27.7
6	14	0.1	7	2	70.6
7	3	0.02	7	8	31.5
8	10	0.1	7	8	89.5
9	12	0.06	4	2	54.5
10	11	0.06	10	2	62.9
11	6	0.06	4	8	67.0
12	1	0.06	10	8	71.9
13	16	0.06	7	5	62.4
14	15	0.06	7	5	58.4
15	8	0.06	7	5	62.9
16	4	0.06	7	5	62.9
17	2	0.06	7	5	66.9

where, V (L) is the volume of CV dye solution, and W (g) is the weight of OPFAC.

2.5. Adsorption kinetic, isotherm, and thermodynamic study

The non-linear pseudo-first-order (PFO) (Eq. (5)) and pseudo-second-order (PSO) (Eq. (6)) models were used to investigate the adsorption kinetic of CV dye on OPFAC surface.

$$q_t = q_e(1 - \exp^{-k_1 t}) \quad (5)$$

$$q_t = \frac{q_e^2 k_2 t}{1 + q_e k_2 t} \quad (6)$$

where q_e (mg/g), q_t (mg/g) are the amount of CV dye adsorbed onto OPFAC per unit mass of activated carbon at equilibrium and at any time t (min). k_1 (1/min) and k_2 (g/mg min) are the rate constant of pseudo-first-order and pseudo-second-order, respectively.

The adsorption isotherm study explains the molecule interaction with the surface of adsorbent. The equilibrium data were fitted using non-linear regression of Langmuir (Eq. (7)), Freundlich (Eq. (8)), and Temkin (Eq. (9)) models.

$$q_e = \frac{q_{\text{max}} K_a C_e}{1 + K_a C_e} \quad (7)$$

$$q_e = K_F C_e^{1/n} \quad (8)$$

$$q_e = \frac{RT}{b_T} \ln(K_T C_e) \quad (9)$$

where, q_e (mg/g) is represent the amount of CV dye adsorbed at equilibrium, C_e (mg/L) is the concentration of CV dye at equilibrium, q_{\max} (mg/g) represent the maximum adsorption capacity, and K_a (L/mg) is Langmuir constant. K_F (mg/g) (L/mg) $^{1/n}$ is the Freundlich constant, n is the dimensionless constant.

For the thermodynamic study, the method followed method as described by Ghibate, Senhaji [10]. The optimum conditions were used in the thermodynamic study. 0.1g of OPFAC was placed into a 250 mL conical flask. Then, 100 mL of CV with 100 ppm and initial pH 9 were added into the flask. After that, the flask was placed in the water bath at different temperatures (25°C 35°C, 45°C, and 55°C) and the solution was filtered out at 3, 4, and 5 min using a syringe filter. The concentration of CV dye removal was measured by UV-Vis spectroscopy at λ_{\max} 590 nm. The thermodynamic was calculated following Eq. (10):

$$\ln k_d \frac{\Delta S^\circ}{R} - \frac{\Delta H^\circ}{RT} \quad (10)$$

Gibbs free energy charge ΔG° was calculated with Eq. (11):

$$\Delta G^\circ = -RT \ln k_d \quad (11)$$

where R is the universal gas constant (8.314 J/mol K), and T is the actual temperature (K), K_d represents the adsorption distribution constant (L/mg) that was analyzed with Eq. (12):

$$k_d = \frac{C_{Ae}}{C_e} \quad (12)$$

where C_{Ae} is the amount of CV dye adsorbed on the adsorbent at equilibrium (mg/L) and C_e is the CV dye at equilibrium(mg/L).

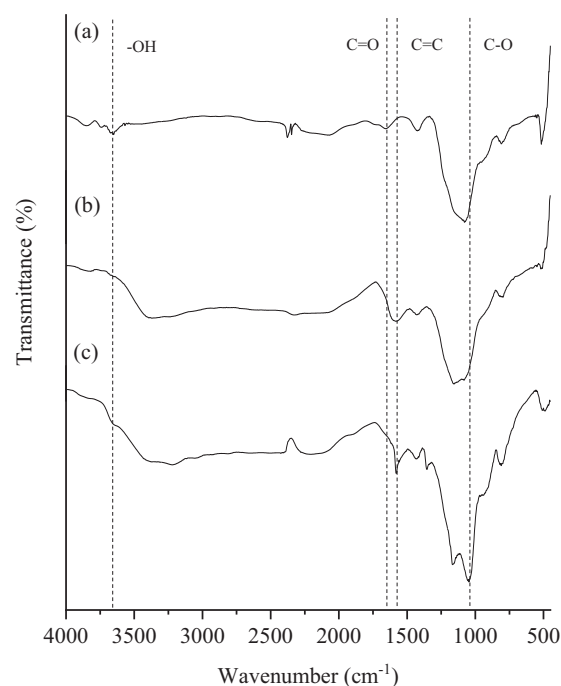
3. Results & discussion

3.1. BET surface area analysis

The BET surface area of OPFAC was 1346.5 m²/g with an average pore width of 4.46 nm and pore volume of 0.936 cm³/g. Activation with phosphoric acid has produced a more porous carbon compared to that of OPF biochar (BET surface area 980.8 m²/g) [11].

3.2. FT-IR analysis

The FT-IR spectra of OPFAC before and after adsorption with CV were shown in the Fig. 1. The FT-IR spectrum of raw OPF shows a band at 1500 cm⁻¹,



(a) Raw OPF (b) OPFAC (Before adsorption) (c) OPFAC (After adsorption)

Fig. 1. FT-IR spectra of (a) raw OPF, (b) OPFAC before and (c) after adsorption of CV.

indicating the presence of C=C bonds of aromatic ring. Another band at 3500 to 3700 cm⁻¹ describes the presence of hydroxyl (-OH) group. The FT-IR spectrum of OPFAC show presence of P-O-P (acid phosphate esters) stretching vibration at 1080 cm⁻¹ and C-O stretching vibration of esters, alcohols, ethers and phenols at 1050 cm⁻¹ [3]. The FT-IR spectrum of OPFAC after adsorption of CV dye did not display much difference compared with that of OPFAC before adsorption. There is slightly shifting of some bands due to the presence of the functional group of OPFAC composite in the CV dye adsorption process [12]. Thus, the band at 1500 cm⁻¹ of CV dye adsorbed on the surface of OPFAC.

3.3. SEM analysis

Figs. 2 and 3 show the surface morphology of OPFAC before and after CV dye adsorption. The shape of OPFAC shows that it has a sponge-like heterogeneous surface related with various pores and cavities. The SEM image of OPF with similar magnification factor has been reported by Sizerici, Fseha [13]. The pore structure of the OPF was not yet developed as expected from any oven-dried biomass. The pore structure was developed after the activation process. The formation of pores associate with the evaporation loss of the activator from the adsorbent surface during activation process [14]. The pores created on the

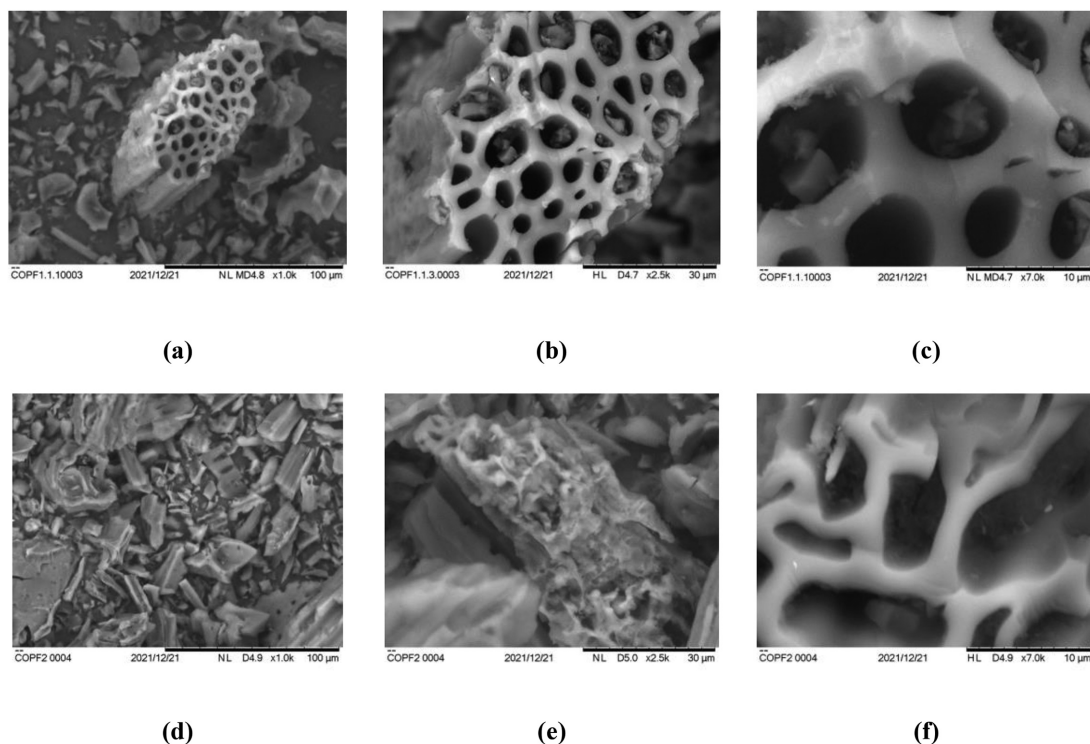


Fig. 2. SEM images of OPFAC at (a) 1000x, (b) 2500x, (c) 7000x magnification and OPFAC after adsorption of CV at (d) 1000x, (e) 2500x, (f) 7000x magnification.

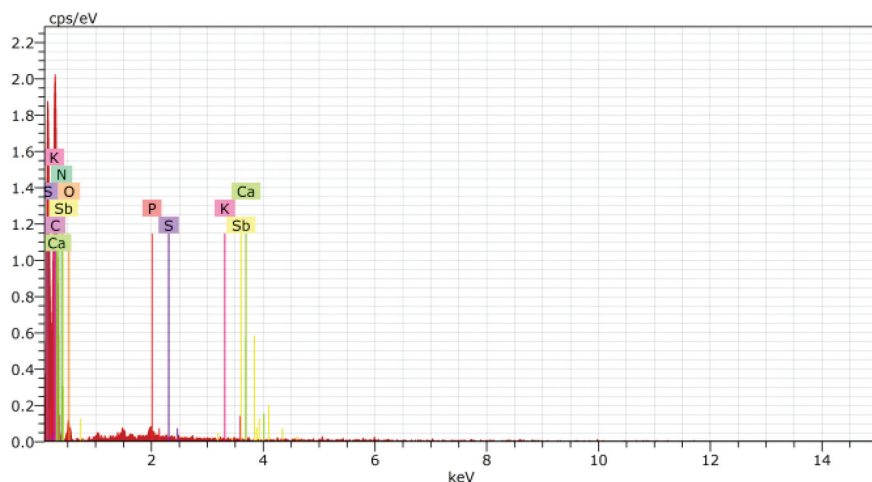


Fig. 3. EDX spectra of OPFAC.

OPFAC surface are categorized as mesopores as the size of cavity is in the range of $1 \mu\text{m}$ to $25 \mu\text{m}$. After the adsorption of CV dye on the surface of OPFAC, the structure is denser with less pores. This indicated that the CV dye has interaction between surface of OPFAC and some of pore of OPFAC were collapse during drying process [15].

Fig. 3 shows EDX analysis of OPFAC contains the element of carbon (C), oxygen (O), phosphorus (P), and sulfur (S). The presence of C describes the present of unburned carbon in the OPFAC. Carbon is important

element in the adsorption process. The EDX show the results OPFAC contain phosphorus, this indicate that the presence of phosphorus in the OPFAC is because of the presence of phosphate and polyphosphate after activation with phosphoric acid (H_3PO_4) [16].

3.4. Thermogravimetric analysis (TGA)

Fig. 4 shows the thermogravimetric analysis (TGA) of raw OPF. The initial weight loss from 50°C to 100°C was due to the water loss in lignocellulosic

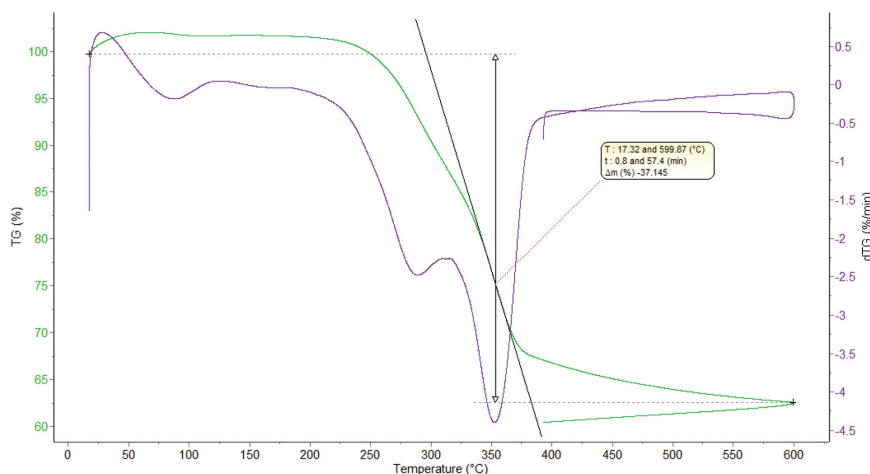


Fig. 4. Thermal gravimetric analysis (TGA) of raw oil palm frond powder.

biomass. The weight loss occurred at temperature 150°C to 250°C was due to depolymerization of lignin and hemicelluloses and the breakdown of glycosidic linkages [17]. The degradation of the α -cellulose was found in the OPF biomass at temperature 300°C to 350°C. The degradation temperature shows difference between top, middle, and bottom part. The bottom part shows more resistance compared to top and middle part. This is due the presence of a higher amount of crystalline structure in the OPF sample [17, 18]. The maximum mass loss of OPF is 37.15% from 17.32°C to 599.9°C due to the release of volatile matter. The rate of mass loss becomes stable when the temperature reaches 600°C. Om Prakash, Raghavendra [19] stated that lignin is the final component to degrade and it directly leads to the creation of carbon formation.

3.5. Point of zero charge (pH_{pzc})

Fig. 5 shows the curve of pH change as a function of the initial pH of the OPFAC aqueous solution. The pH_{pzc} of OPFAC was 6.5. This indicates that the surface charge of the OPFAC is electrostatically neutral. The OPFAC would possess a positive charge surface if solution $\text{pH} < \text{pH}_{\text{pzc}}$ [20]. At a $\text{pH} > 6.5$, the surface of OPFAC would be negative charge. This shows the ability of cationic CV dye to attach to OPFAC. Therefore, high electrostatic interaction between negatively charged of OPFAC and cationic CV dye can be obtained as shown in Fig. 6.

3.6. Optimization study

Based on the ANOVA analysis in Table 3, the F-value (66.94) of the model corresponds with p-value (<0.0001). The values indicate that the model is

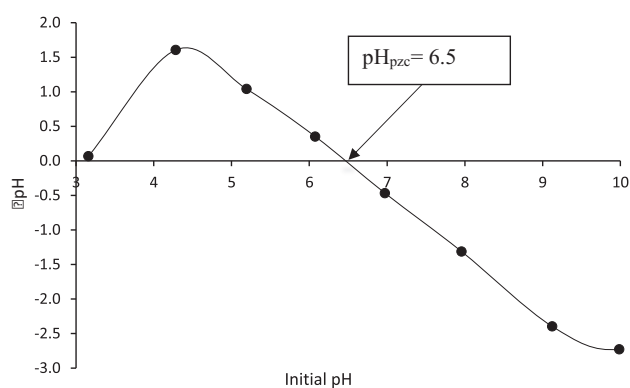


Fig. 5. The point of zero charge (pH_{pzc}) of the OPFAC.

significant [12]. For CV dye removal, the model regression coefficient of determination, R^2 was 0.9885, which is consistent with the experimental results as the difference is less than 0.2. This indicates that the results show a high correlation between actual and predicted values.

The final expected process models in terms of the actual significant factor for the percentage of CV dye removal are recorded in Eq. (13):

$$\begin{aligned} \text{CV removal (\%)} = & +63.10 + 25.00 A + 5.18 B \\ & + 5.53 C - 5. + 3.78 AC - 0.8750 BC - 3.86 A^2 \\ & + 5.39 B^2 - 4.41 C^2 \end{aligned} \quad (13)$$

It can be concluded that the A, B, C, AC, and B^2 are significant (p-value < 0.0500) and had positive impact on the CV dye removal by OPFAC.

Graphical approaches (Fig. 7) have been used to evaluate the BBD model and analyse the nature of the residual distribution and the association between the actual and expected CV dye removal rates. Fig. 7(a)

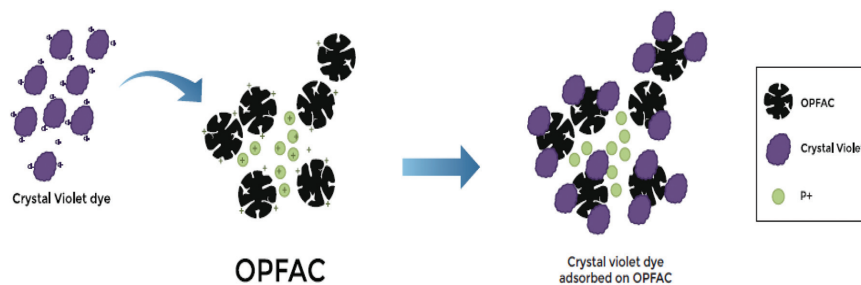


Fig. 6. Negative charge of OPFAC with cationic CV dye.

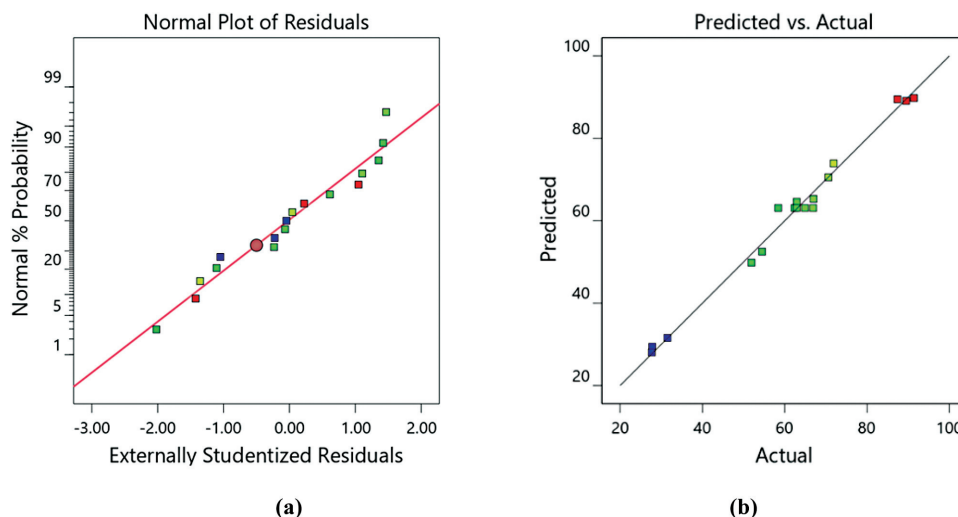


Fig. 7. (a) Graph of normal probability of CV dye removal residuals, (b) plot of the relationship between predicted and actual values of CV dye removal (%).

Table 3. Analysis of variance (ANOVA) for the removal of CV dye.

Source	Sum of Squares	Df	Mean Square	F-value	p-value
Model	5875.14	9	652.79	66.94	<0.0001
A-Dose	5000.00	1	5000.00	512.71	<0.0001
B-pH	214.25	1	214.25	21.97	0.0022
C-Time	244.20	1	244.20	25.04	0.0016
AB	101.00	1	101.00	10.36	0.0147
AC	57.00	1	57.00	5.85	0.0463
BC	3.06	1	3.06	0.3140	0.5927
A ²	62.82	1	62.82	6.44	0.0388
B ²	122.21	1	122.21	12.53	0.0095
C ²	81.98	1	81.98	8.41	0.0230
Residual	68.27	7	9.75		
Lack of Fit	27.97	3	9.32	0.9252	0.5056
Pure Error	40.30	4	10.08		
Cor Total	5943.40	16			

shows the perfect normal distribution of the residuals and has been seen as a point remarkably close to a straight line. Thus, it indicates that the assumption and independence of the residuals are accurate. The correlation between actual and predicted CV dye removal rates (Fig. 7(b)) shows that the actual and predicted values in the BBD model's statistical evaluation are in good correlation.

Fig. 8(a) shows that dosage (A) and pH (B) are of statistical significance (p -value <0.0001) and have a positive effect on OPFAC removal of CV dye. The percentage removal of CV dye was increased by increasing the dosage of OPFAC and solution pH from 4 to 10. Consistent with findings from Fig. 8(b), a higher solution pH increased negative charge of OPFAC, causing an increase of adsorption sites and surface area for the cationic species of the CV dye to attach. Fig. 8(c) shows the response surface plot of the Dose (A) and time (C). The correlation between dosage and contact time is significant, and it has a positive effect on the CV dye removal. Fig. 8(d) is the 3D response surface plot of the AC interaction. The percentage of the CV dye removal increased by increasing the OPFAC dose. This is due to the fact that in the bulk solution of CV dye, a larger number of active adsorption sites and surface area of OPFAC will be exposed to the CV dye [15].

3.7 Sorption study

Fig. 9 shows the adsorption capacity, q_t (mg/g) as a function of contact time (min) at various initial CV

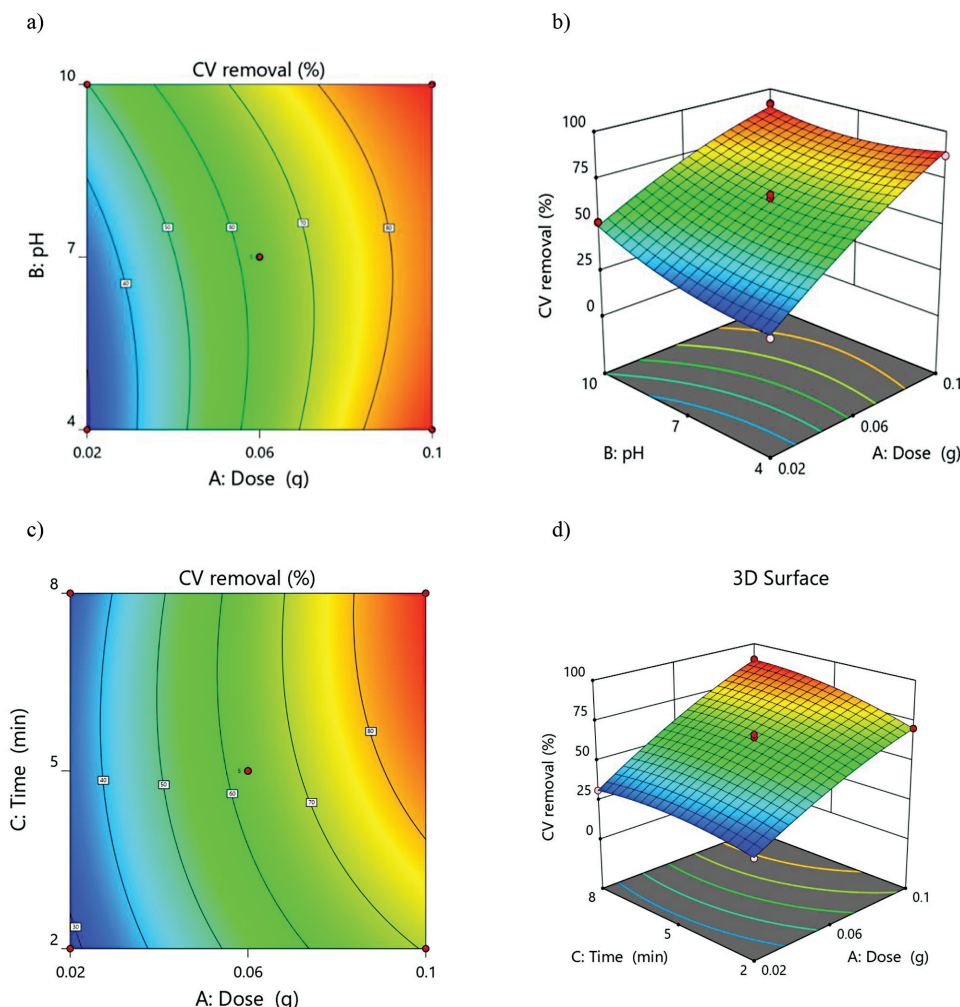


Fig. 8. 3D response surface plots of CV dye removal show the interaction between (a & b) dosage and pH; whereas, (c & d) shows the interaction between dosage and time.

dye concentrations (50, 100, 150, 200, 250 and 300 mg/L). The results stipulate that by increasing the initial concentration from 50 to 300 mg/L, the quantity of CV dye molecules adsorbed onto the surface of the OPFAC increased from 45.42 mg/L to 231.47 mg/L. The results are attributed to the relatively high concentration gradient, which enhances CV dye adsorption and movement to the active adsorption sites inside OPFAC's micropore as a high concentration gradient provide a driving force [3, 12].

3.8. Adsorption kinetic study

Table 4 shows PFO and PSO kinetic parameters for CV dye adsorption on OPFAC. The adsorption of CV dye by OPFAC follows the PSO model due to the higher correlation coefficient ($R^2 \geq 0.99$) than that of the PFO model. This indicates that the adsorption of CV dye by OPFAC was of a chemisorption process,

i.e., electrostatic interaction between the negatively-charged surface of the OPFAC and the cationic CV dye [12].

3.9. Adsorption isotherm study

Fig. 10 shows plots of nonlinear isotherm and Table 5 display the parameters of various adsorption isotherm models. The results indicate that the adsorption of CV by OPFAC is best described by the Freundlich model ($R^2 = 0.9488$) compared to Langmuir ($R^2 = 0.7455$) and Temkin models ($R^2 = 0.8988$). This indicated that the adsorption occurred through multilayer CV dye adsorption onto the heterogeneous adsorption site of the OPFAC. The adsorption capacity (q_m) of OPFAC for CV dyes was 188.4 mg/g and is higher than other oil palm derived sorbents, such as the oil palm frond magnetic biochar (149.03 mg/g) [11], palm kernel shell-phosphoric

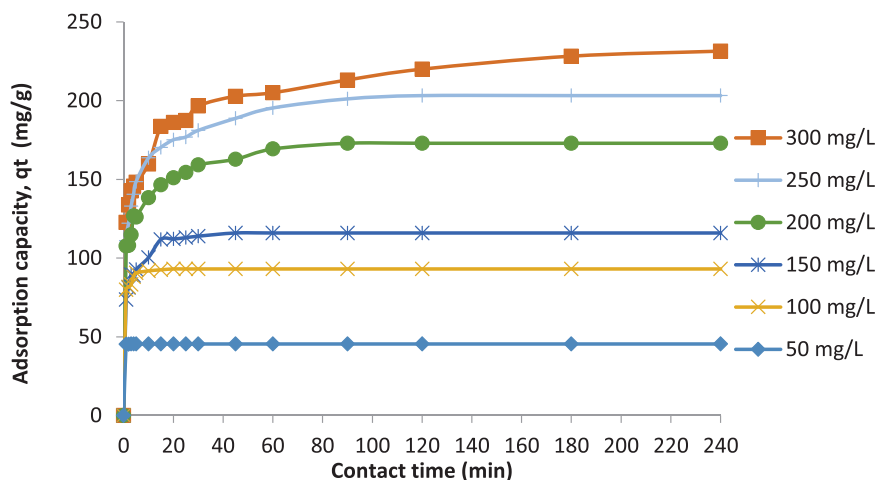


Fig. 9. CV adsorption capacity (mg/g) by OPFAC as a function of contact time (min) at various initial CV concentration (mg/L).

Table 4. PFO and PSO kinetic parameters for CV dye adsorption on OPFAC.

Concentration (mg/L)	Pseudo-first-order (PFO)				Pseudo-second-order (PSO)		
	$q_e \text{ exp}$ (mg/g)	$q_e \text{ cal}$ (mg/g)	k_1 (1/min)	R^2	$q_e \text{ cal}$ (mg/g)	$k_2 \times 10^{-2}$ (g/mg min)	R^2
50	45.42	45.41	5.842	1.000	45.43	6.780	1.000
100	93.08	91.39	1.845	0.9793	93.25	0.05079	0.9956
150	115.9	111.1	0.6744	0.9174	115.5	0.01074	0.9804
200	172.9	158.4	0.5734	0.8599	165.7	0.005972	0.9481
250	203.2	185.3	0.4935	0.8881	194.2	0.004242	0.9639
300	231.5	198.7	0.4765	0.8268	209.6	0.00359	0.9257

Table 5. Parameters of the Langmuir, Freundlich, and Temkin isotherm models for CV dye adsorption on OPFAC.

Adsorption isotherm	Parameters	Value
Langmuir	q_m (mg/g)	188.4
	K_a (L/mg)	1.391
	R^2	0.7455
Freundlich	K_f (mg/g) (L/mg) ^{1/n}	79.55
	n	4.195
	R^2	0.9488
Temkin	K_T	40.28
	b_T (J/mol)	97.85
	R^2	0.8988

acid activated carbon (81.30 mg/g) [21]. and palm kernel shell biochar (24.45 mg/g) [22].

3.10. Thermodynamic study

A Plot of $\ln k_d$ versus $1/T$ was illustrated in Fig. 11. It shows a linear relationship with ΔH° and ΔS° identified from the slope and intercept, respectively. The CV dye adsorption thermodynamic parameters on OPFAC is shown in Table 6. The negative values of ΔG° (−5.314, −5.921, and −7.084 KJ/mol) indicate that the adsorption process is a favourable and spontaneous with high sorption preference of CV dye onto OPFAC. The values of ΔG° were decreasing

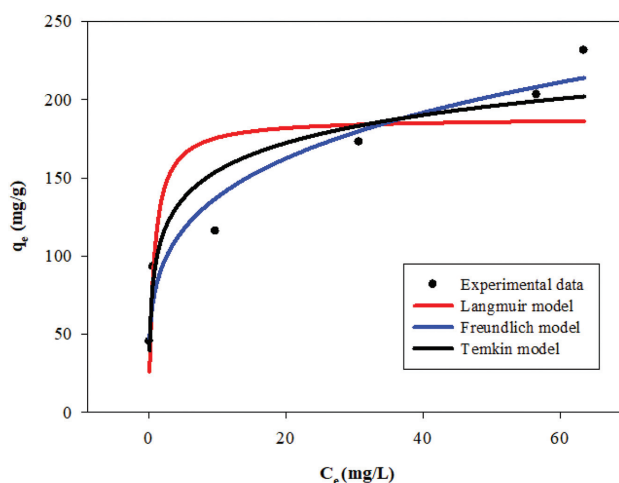


Fig. 10. Adsorption isotherm of CV dye by OPFAC (adsorbent dose 0.1g and pH of solution = 9, agitation speed = 150 strokes/min and volume of solution = 100 mL).

as the temperature rises, indicating that the adsorption process is encouraged by higher temperatures [23]. Meanwhile, the positive value of ΔH° (21.86 KJ/mol) indicates that the CV dye adsorption by the OPFAC is an endothermic process. Furthermore, the ΔS° value is positive (87.90 J/mol K), suggesting

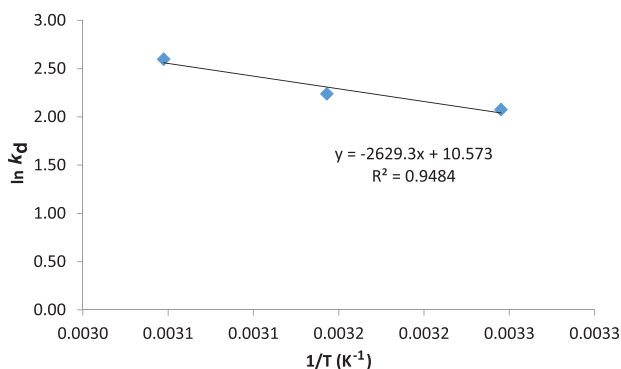


Fig. 11. Van't Hoff plot for the adsorption of CV dye on OPFAC.

Table 6. Thermodynamic parameters values for the adsorption of CV dye by OPFAC.

T (K)	ΔG° (KJ/mol)	ΔH° (KJ/mol)	ΔS° (J/mol K)
308.2	-5.314	21.86	87.90
318.2	-5.921		
328.2	-7.084		

that the randomness at the solid-liquid interface has increased during the adsorption process.

4. Conclusion

This study has successfully converted OPF into mesoporous activated carbon using microwave pyrolysis and activation with H_3PO_4 . It reveals that OPFAC can be a renewable and potential adsorbent for removing CV dye from an aqueous environment. The characteristic of OPFAC was conducted by using FT-IR, SEM analysis and pH_{pzc} . The point of zero charge (pH_{pzc}) of OPFAC were observed at $pH = 6.974$. The Box-Behnken design (BBD) indicated that 0.1 g adsorbent dose, solution adjusted pH 9 and contact time 5 mins were the best OPFAC adsorption condition for CV dye removal. The adsorption kinetic analysis showed that pseudo-second-order (PSO) is the best-fitted model. Besides, the adsorption isotherm is well described by the Freundlich model with the maximum adsorption capacity (q_m) 188.4 mg/g. The thermodynamics study indicated that the adsorption process of OPFAC is through spontaneous and endothermic condition as the values of ΔH° (21.86 KJ/mol) and ΔS° value (87.90 J/mol K) is positive. Cation exchanged capacities (CEC) analysis is recommend in the further studies in order to measure exchangeable cations that OPFAC can be adsorb. For the adsorption study, it is recommended that the adsorption isotherm to be analyzed with the Dubinin-Radushkevich model to explain the adsorption mechanism with a Gaussian energy distribution on a heterogeneous surface.

Acknowledgment

Authors acknowledge the IIUM-UIMP-UiTM Sustainable Research Collaboration Grant 2020 (SRCG) 600-RMC/SRC/5/3 (030/2020).

Conflicts of interest

Authors declare no conflicts of interest.

References

- Zhao Q, Yu L, Li X, Xu Y, Du Z, Kanniah K, et al. The expansion and remaining suitable areas of global oil palm plantations. *Global Sustainability*. 2024;7:e9.
- Saharudin DM, Jeswani HK, Azapagic A. Bioenergy with Carbon Capture and Storage (BECSS): life cycle environmental and economic assessment of electricity generated from palm oil wastes. *Applied Energy*. 2023;349:121506.
- Jawad AH, Mohd Firdaus Hum NN, Abdulhameed AS, Mohd Ishak MA. Mesoporous activated carbon from grass waste via H_3PO_4 -activation for methylene blue dye removal: modelling, optimisation, and mechanism study. *International Journal of Environmental Analytical Chemistry*. 2020:1–17.
- Maulina S, Handika G. Characteristics of activated carbon from oil palm fronds with the addition of sodium carbonate (Na_2CO_3) and sodium chloride (NaCl) as an activator. *Simetrikal: Journal of Engineering and Technology*. 2019;1(1):30–35.
- Puri C, Sumana G. Highly effective adsorption of crystal violet dye from contaminated water using graphene oxide intercalated montmorillonite nanocomposite. *Applied Clay Science*. 2018;166:102–112.
- Foong SY, Chan YH, Yek PNY, Lock SSM, Chin BLF, Yiin CL, et al. Microwave-assisted pyrolysis in biomass and waste valorisation: insights into the Life-Cycle Assessment (LCA) and Techno-economic Analysis (TEA). *Chemical Engineering Journal*. 2024;491:151942.
- Heidarinejad Z, Dehghani MH, Heidari M, Javedan G, Ali I, Sillanpää M. Methods for preparation and activation of activated carbon: a review. *Environmental Chemistry Letters*. 2020;18(2):393–415.
- Inyang M, Dickenson E. The potential role of biochar in the removal of organic and microbial contaminants from potable and reuse water: a review. *Chemosphere*. 2015;134:232–240.
- Mahdi Z, Hanandeh AE, Yu Q. Influence of pyrolysis conditions on surface characteristics and methylene blue adsorption of biochar derived from date seed biomass. *Waste and Biomass Valorization*. 2016;8(6):2061–2073.
- Ghibate R, Senhaji O, Taouil R. Kinetic and thermodynamic approaches on rhodamine B adsorption onto pomegranate peel. *Case Studies in Chemical and Environmental Engineering*. 2021;3:100078.
- Oyekanmi AA, Katibi KK, Omar RC, Ahmad A, Elbidi M, Alshammari MB, et al. A novel oil palm frond magnetic biochar for the efficient adsorption of crystal violet and sunset yellow dyes from aqueous solution: synthesis, kinetics, isotherm, mechanism and reusability studies. *Applied Water Science*. 2024;14(2):13.
- Jawad AH, Malek NNA, Abdulhameed AS, Razuan R. Synthesis of magnetic chitosan-fly ash/ Fe_3O_4 composite for adsorption of reactive orange 16 dye: optimization by

- box-behnken design. *Journal of Polymers and the Environment*. 2020;28(3):1068–1082.
13. Sizirici B, Fseha YH, Yildiz I, Delclos T, Khaleel A. The effect of pyrolysis temperature and feedstock on date palm waste derived biochar to remove single and multi-metals in aqueous solutions. *Sustainable Environment Research*. 2021;31(1):9.
 14. Ao W, Fu J, Mao X, Kang Q, Ran C, Liu Y, et al. Microwave assisted preparation of activated carbon from biomass: a review. *Renewable and Sustainable Energy Reviews*. 2018;92:958–979.
 15. Jawad AH, Abdulhameed AS. Statistical modeling of methylene blue dye adsorption by high surface area mesoporous activated carbon from bamboo chip using KOH-assisted thermal activation. *Energy, Ecology and Environment*. 2020;5(6):456–469.
 16. Romero-Anaya AJ, Molina A, Garcia P, Ruiz-Colorado AA, Linares-Solano A, Salinas-Martínez de Lecea C. Phosphoric acid activation of recalcitrant biomass originated in ethanol production from banana plants. *Biomass and Bioenergy*. 2011;35(3):1196–1204.
 17. Nordin NA, Sulaiman O, Hashim R, Mohamad Kassim MH. Characterization of different parts of oil palm fronds (*Elaeis Guineensis*) and its properties. *International Journal on Advanced Science, Engineering and Information Technology*. 2016;6(1):74–76.
 18. Ouajai S, Shanks RA. Morphology and structure of Hemp fibre after bioscouring. *Macromol Biosci*. 2005;5(2):124–134.
 19. Om Prakash M, Raghavendra G, Ojha S, Panchal M. Characterization of porous activated carbon prepared from arhar stalks by single step chemical activation method. *Materials Today: Proceedings*. 2021;39:1476–1481.
 20. Kragović M, Stojmenović M, Petrović J, Loredo J, Pašalić S, Nedeljković A, et al. Influence of alginate encapsulation on point of zero charge (pHpzc) and thermodynamic properties of the natural and Fe(III)-modified zeolite. *Procedia Manufacturing*. 2019;32:286–293.
 21. Buhani B, Suharso S, Luziana F, Rilyanti M, Sumadi S. Production of adsorbent from activated carbon of palm oil shells coated by Fe₃O₄ particle to remove crystal violet in water. *Desalination and Water Treatment*. 2019;171:281–293.
 22. Kyi PP, Quansah JO, Lee C-G, Moon J-K, Park S-J. The removal of crystal violet from textile wastewater using palm kernel shell-derived biochar. *Applied Sciences*. 2020;10(7):2251.
 23. Jawad AH, Bardhan M, Islam MA, Islam MA, Syed-Hassan SSA, Surip SN, et al. Insights into the modeling, characterization and adsorption performance of mesoporous activated carbon from corn cob residue via microwave-assisted H₃PO₄ activation. *Surfaces and Interfaces*. 2020;21:100688.